Electrochemical Synthesis and Characterization of Conducting Copolymers of Biphenyl with Pyrrole

Johannis Simitzis, Spyridon Soulis, Despina Triantou

Laboratory Unit "Advanced and Composite Materials," Department III "Materials Science and Engineering," School of Chemical Engineering, National Technical University of Athens, Athens 157 73, Greece

Received 13 January 2011; accepted 3 October 2011
DOI 10.1002/app.36301
Published online 18 January 2012 in Wiley Online Library (wileyonlinelibrary.com).

ABSTRACT: Copolymer films of biphenyl and pyrrole were synthesized by electrochemical polymerization. The influence of the applied potential used for the electropolymerization on the structure, morphology, electrical conductivity, and stability of the films was examined. From the analysis of the current–time curves, it was found that the growth of the copolymer films starts immediately. The films were characterized by Fourier transform infrared spectroscopy (FTIR), thermogravimetric analysis, X-ray diffraction analysis, and scanning electron microscopy–energy-dispersive X-ray analysis, and their electrical conductivity (σ), energy gap (E_g), and electrochemical stability were also determined. Based on the results, the copolymers were classified into three groups. The first includes the $(PP\text{-}PPy)_{0.80}$ copolymer synthesized at the lowest potential E_{ox} (0.80 V), having the highest ratio R ($R = 0.35$) of quinoid to benzenoid rings (calculated from FTIR), the highest value of σ (σ = 0.9 S/cm), the lowest E_g ($E_g = 1.20$ eV), and has compact morphology. The second group concerns the copolymers synthesized at higher potential (0.82 up to 0.86 V), having lower R (∼ 0.20), lower σ (below 0.4 S/cm), higher E_g (∼ 1.35 eV), and they are less compact with many pores. The third group includes the copolymers synthesized at even higher applied potential (0.88 and 0.90 V), having even lower R values (∼ 0.10), significantly lower σ (∼ 10^{-3} S/cm), even higher E_g (∼ 1.70 eV), and they are very porous. The applied potential during electropolymerization strongly affects the properties of the synthesized copolymers. Because of the combination of high conductivity, low energy gap, and partial solubility with significant electrochemical stability, these new copolymers are attractive candidates for many applications. © 2012 Wiley Periodicals, Inc. J Appl Polym Sci 125: 1928–1941, 2012

Key words: conducting polymers; polyphenylene; polypyrroles; copolymerization; electrical conductivity

INTRODUCTION

The research in the field of conducting polymers (CPs) begun in 1970s and remains still active. These materials combine low cost, low density, mechanical flexibility, and easy processability and are used in many electronic (e.g., transistors), electrochemical (e.g., sensors), and electrooptical (e.g., photovoltaic solar cells) applications.[1–5] CPs can be synthesized chemically or electrochemically, having the form of powder or the form of film, respectively. The electropolymerization method exhibits many advantages such as the direct formation of the polymer in the doped state on the electrode surface and the control of the film thickness.[6,7]

Polyphenylenes (PPs) have attracted much interest among various CPs because of their high stability in air even at high temperatures due to the aromatic nuclei.[8–10] PPs have been extensively investigated, particularly as active materials for use in light-emitting diodes (LEDs) and polymer lasers. PPs can be prepared using biphenyl (Biph) or other aromatic compounds leading to isomeric PPs containing both ortho-, meta-, and para-couplings between the aromatic rings.[8,11] Polypyrroles (PPys) are counted among the most stable CPs, whereas polythiophenes exhibit intermediate stabilities.[12] Moreover, the ability of PPy to switch between oxidized and reduced states (i.e., under repetitive potential cycling), leading to conducting or insulating polymer films, is very important, especially for electrochemical and electrooptical applications such as sensors and LEDs.[13]

Apart from the conducting homopolymers, copolymers based on different types of monomers have gained great scientific interest, because new electrically active materials could be produced combining properties of both of the homopolymers.[9,14]. By electrochemical copolymerization, a variety of conducting materials with different electrical and morphological properties can be produced.[10,14]

In our previous work,[10] we studied the synthesis of copolymers based on Biph and thiophene, which were found to combine high conductivity, low energy gap, and high stability under repetitive potential cycling when compared with both PPs and

Correspondence to: J. Simitzis (simj@chemeng.ntua.gr).

polythiophenes. Under this scope, it would be interesting to synthesize copolymers with even better electrochemical stability. As already mentioned, PPys are more stable than polythiophenes. Thus, the aim of this work is to study the electrochemical copolymerization of Biph and pyrrole (Py). These copolymers will be examined with reference to their corresponding homopolymers from the scope of electrical conductivity and their electrochemical stability.

EXPERIMENTAL

Py (Fluka) was vacuum distilled before use. Tetrabutylammonium tetrafluoroborate ($TBABF_4$; Merck, Darmstadt, Germany) was dried at 110°C up to constant weight. Acetonitrile (ACN, water content ~0.05%; Merck, Darmstadt, Germany) was stored over molecular sieves (4 Å, 8–12 mesh; Fluka, Steinheim, Germany) for about 1 month. Biph (Fluka, Steinheim, Germany) was used as received.

The copolymer films based on Biph and Py and the corresponding homopolymers were synthesized by anodic potentiostatic electropolymerization at various constant potentials for 30 min. The electropolymerization solution consisted of the monomers (Biph and/or Py), $TBABF_4$ as supporting electrolyte, and ACN as solvent. The monomers were used with the following concentrations: [Biph]/[Py] = 0.05*M*/0.05*M* for copolymers; [Biph] = 0.1*M* for PP homopolymers; [Py] = 0.1*M* for PPy homopolymers; and the electrolyte concentration was [$TBABF_4$] = 0.1*M*. All electropolymerizations took place at room temperature in an one-compartment electrochemical cell. The analytical experimental procedure has been described in detail in our previous work.[10] The thickness of the films synthesized was estimated from the amount of charge during the electropolymerization. After electropolymerization, the (co)polymers synthesized were immersed in ACN to remove residual monomer(s) or electrolyte and then vacuum dried at 30°C up to constant weight to remove residual solvent.

The solubility of the films synthesized was tested in various common solvents [i.e., ethanol (Et), methanol (Me), acetone (Ac), *N*-methylpyrrolidone (NMP), tetrahydrofuran (THF), *N*,*N*′-dimethylformamide (DMF), chlorobenzene (BzCl), and *N*,*N*′-dimethylsulfoxide (DMSO)]. The Fourier transform infrared (FTIR) spectra of the polymers were recorded using a Perkin–Elmer Spectrum GX spectrometer using KBr discs. The thermogravimetric analysis (TGA) measurements were recorded using a Mettler Toledo 815E thermobalance with aluminum pans by heating the sample from 25 up to 1000°C with a heating rate of 10°C/min under nitrogen flow. The morphology of the films was examined using a FEI Quanta 200 Scanning Electron Microscope (SEM) with simultaneous energy-dispersive X-ray analysis (EDAX). The electrical conductivity of the films with constant current was determined at room temperature by the two-probe technique.[15] The energy levels of the highest occupied molecular orbital (E_{HOMO}) and that of the lowest unoccupied molecular orbital (E_{LUMO}), as well as the energy gap (E_g), were determined by cyclic voltammetry.[10,16]

RESULTS AND DISCUSSION

Synthesis of polymer films

At the beginning of this research, we have studied the electropolymerization in four different electrolytes ($TBABF_4$, tetrabutylammonium hexafluorophosphate, tetrabutylammonium perchlorate, and lithium perchlorate) and three different solvents (ACN, propylene carbonate, and nitrobenzene). Based on the properties of the films synthesized (e.g., morphology, electrical conductivity, and stability), the system of $TBABF_4$ with ACN was chosen as the most appropriate system. For the selected system, the effect of the concentration of the monomer and that of the electrolyte on the properties of the polymers has been investigated. The most appropriate concentration for monomer and electrolyte is 0.1*M* in ACN. Concerning the copolymers, the concentration ratio of Biph to Py varied as follows: Biph/Py = 0.025*M*/0.075*M*, 0.05*M*/0.05*M*, and 0.075*M*/0.025*M*; the ratio of 0.05*M*/0.05*M* led to films with the best properties.

To synthesize the copolymer films, the oxidation potential (E_{ox}) of the combination of the monomers should be known, as this is the minimum potential where copolymerization could take place. The experimental procedure for the determination of E_{ox} has been described in our previous work.[10] For the Biph–Py monomer system, the E_{ox} is 0.80 V (vs. Saturated Calomel electrode, SCE). The E_{ox} values of Biph and Py in the defined electropolymerization solution is 1.80 and 0.80 V (vs. SCE), respectively, which are in accordance with the literature.[8,17]

To investigate the effect of the applied potential on the properties of the polymer films, electropolymerizations were carried out at potentials from E_{ox} (V) up to E_{ox} + 0.1 (V), with an increase step of 0.02 V. The synthesized films were macroscopically examined, and those that were inhomogeneous were discarded. Thus, only the films synthesized under the chosen potentials (which lead to homogeneous films) will be considered. Table I presents the raw materials, the experimental parameters for the synthesis of the films, the total charge, and the characteristics (thickness, color, and soluble fraction in NMP, DMF, and DMSO) of synthesized polymeric films. From Figure 1, the total charge and the

TABLE I
Raw Materials, Experimental Parameters for the Synthesis of the Films, Charge, and Characteristics of Synthesized Polymeric Films

	Synthesis of the films				Characteristics of films synthesized					
	Raw materials		Experimental parameters							
	Monomers						Soluble fraction (in % w/w) to the initial amount of polymer			
Code of polymers	Biphenyl (mol/L)	Pyrrole (mol/L)	Applied potential for 30 min (V vs. SCE)	Total charge (mC/cm^2)	Thickness (μm)	Color	NMP	DMF	DMSO	Degree of crystallinity x_c (%)
Homopolymers										
$PP_{1.80}$	0.1	–	1.80	821.6	5.8	Dark brown	100	0	0	0
$PP_{1.82}$			1.82	796.9	5.6	Dark brown				0
$PP_{1.84}$			1.84	578.0	4.0	Dark brown				0
$PPy_{0.84}$	–	0.1	0.84	380.6	0.9	Black	0	0	0	0
$PPy_{0.86}$			0.86	524.9	1.3	Black				15.0
$PPy_{0.88}$			0.88	699.9	1.8	Black				22.5
$PPy_{0.90}$			0.90	814.4	2.0	Black				32.4
Copolymers										
$(PP\text{-}PPy)_{0.80}$	0.05	0.05	0.80	130.1	0.6	Black	0	21.0	10.0	30.0
$(PP\text{-}PPy)_{0.82}$			0.82	191.4	0.9	Black		23.5	12.5	23.4
$(PP\text{-}PPy)_{0.84}$			0.84	281.6	1.3	Black		27.5	13.5	12.8
$(PP\text{-}PPy)_{0.86}$			0.86	325.4	1.5	Black		30.0	20.0	0

Supporting electrolyte: tetrabutylammonium tetrafluoroborate, 0.1*M*; solvent: acetonitrile. Results of polyphenylenes $PP_{1.80}$, $PP_{1.82}$, and $PP_{1.84}$ are taken from Ref. 10.

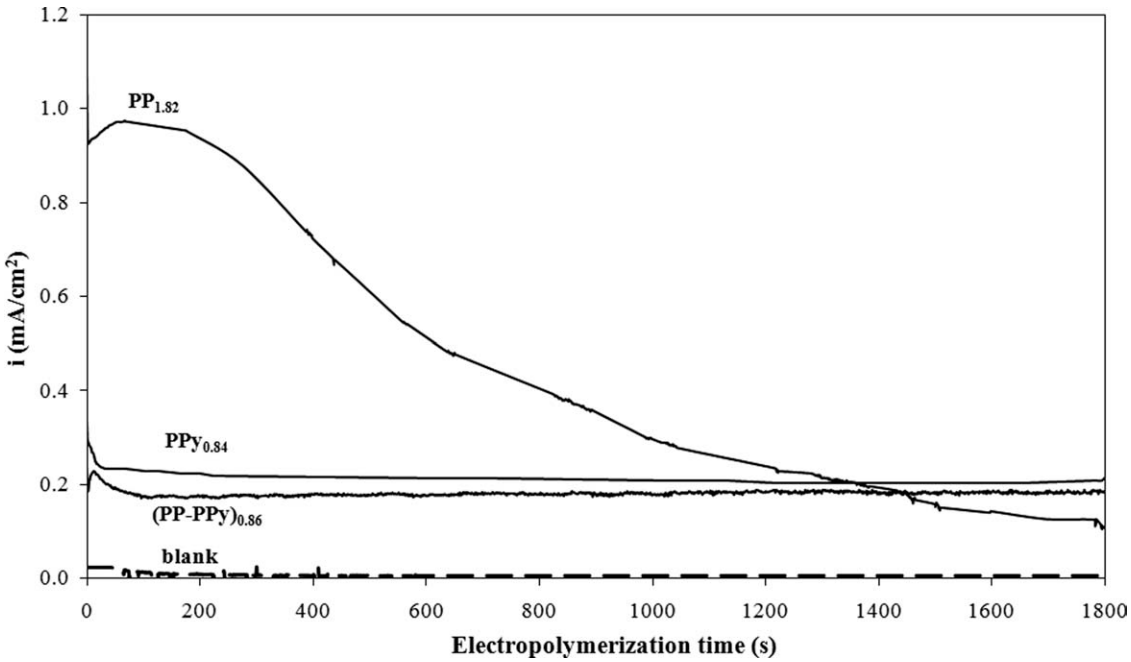

Figure 1 Current versus time for blank solution, homopolymers $PP_{1.82}$ and $PPy_{0.84}$, and copolymer $(PP\text{-}PPy)_{0.86}$ (for the codes, see Table I).

thickness of films can be determined. This figure shows the current (i) and time (t) curves for the electropolymerization of the representative homopolymers $PP_{1.82}$ and $PPy_{0.84}$ and the copolymer $(PP\text{-}PPy)_{0.86}$. In Figure 1, the (i)–(t) curve of blank solution (i.e., the same solution as that of electropolymerization without monomers) at 0.86 V is also presented. By comparing the curve of blank solution with those during electropolymerization, it is obvious that the current measured is due to the reaction of electropolymerization. The thickness of a film can be estimated from the corresponding charge[10,18] on the basis that the synthesis of a PP film with thickness of 1 μm requires 142.8 mC/cm^2 (Q_{PP}),[18] whereas the synthesis of PPy requires 400 mC/cm^2 (Q_{PPy}).[18,19] The corresponding charge required for the synthesis of a 1-μm thick copolymer film is not available in the literature and it was estimated as the harmonic mean of Q_{PP} and Q_{PPy}[10]:

$$Q_{PP-PPy} = (2 \times O_{PP} \times Q_{PPy})/(Q_{PP} + Q_{PPy}) \quad (1)$$

Thus, $Q_{PP\text{-}PPy} = 210.5$ mC/cm^2. The thickness of the copolymers and PPy is lower than that of PPs (Table I, column 6). The copolymers and PPy films synthesized had black color, whereas PPs had dark brown (Table I, column 7).

Electropolymerization mechanism

The (i)–(t) curves were analyzed based on the electropolymerization mechanism described in the literature.[8,10,20–23] According to Figure 1, the shape of the (i)–(t) curve of PP is completely different than that of PPy. The corresponding curve of the copolymer resembles to that of PPy. Based on the literature,[8,20–23] the basic reaction steps take place between $t = 0$ s and $t = 300$ s. Therefore, the initial part of the (i)–(t) curve of the copolymer $(PP\text{-}PPy)_{0.86}$ is presented in Figure 2. According to detailed analysis presented in our previous work[10] and the literature therein, the experimental curves are separated in regions and subregions as follows:

- Region I: Charging of the interface between the working electrode and the electrolytic solution due to the applied potential. After charging, the monomers are adsorbed onto the interface and they oxidize to radical cation form.
- Region II: Nucleation to initiate the electropolymerization and growth of the polymer. Specifically, in this region, two radical cations (which were formed during Region I) are bonded together or a radical cation with a monomer. Following the progress of the reaction, oligomers are formed containing two to five aromatic rings.
- Region III (III_a and III_b): The growth of the already mentioned nuclei continues (Region III_a), but with smaller rate than that of Region II. After a certain time, the growth rate is stabilized and the film is formed, resulting in a current plateau (Region III_b).
- Region IV (IV_a and IV_b): This region refers to macroscopic phenomena, as the film has been formed and its growth continues. More specifically, in Subregion IV_a, the growth rate of the

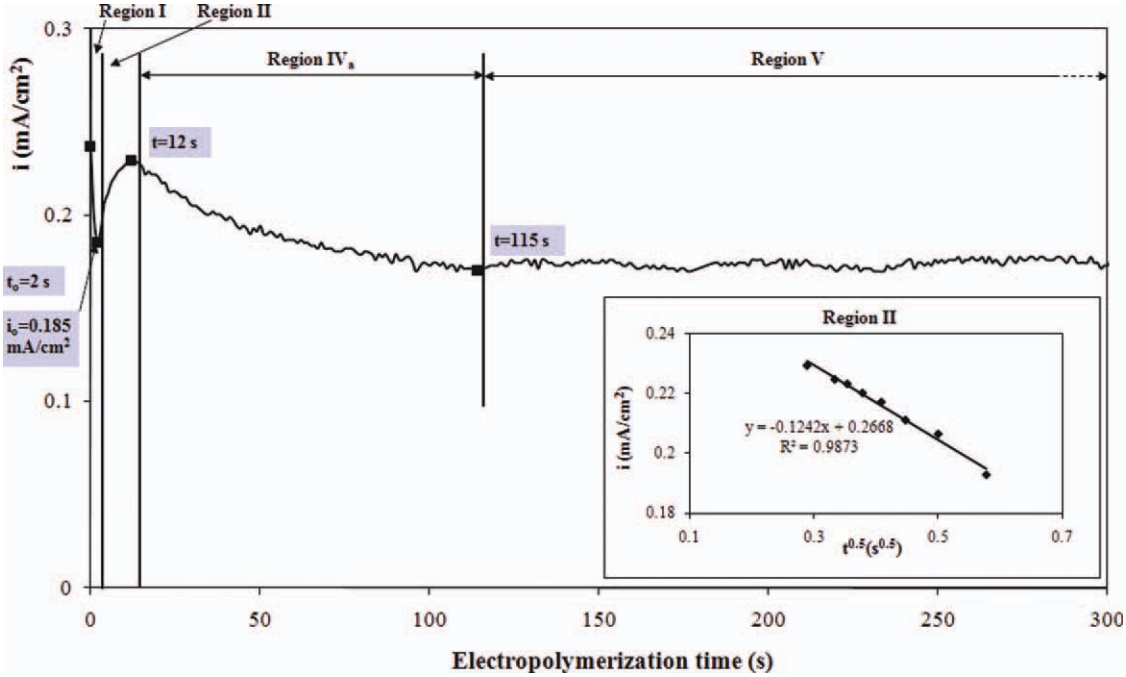

Figure 2 Current versus electropolymerization time from 0 up to 300 s for copolymer $(PP\text{-}PPy)_{0.86}$ (for the code, see Table I). [Color figure can be viewed in the online issue, which is available at wileyonlinelibrary.com.]

film decreases because of the overlapping of the growing nuclei and the diffusion of the radical cation to the electrolytic solution (i.e., they do not take part any more in the film growth). In Subregion IV_b, a loosely adhered layer is formed, above the already formed, compact film.

- Region V: Film growth continues with a state rate.

PPs do not show the Subregion IV_b; PPys do not show the Regions III and IV_b; and copolymers generally do not show the Regions II and III. Subregion IV_b is undesirable, given that it leads to inhomogeneous films. This subregion appeared in the case of $(PP\text{-}PPy)_{0.82}$ and $(PP\text{-}PPy)_{0.84}$; however, it was short (33 and 77 s, respectively) and did not affect the uniformity of the films (as macroscopically observed).

The nucleation and growth mechanism (NGM) can be determined from the analysis of Region II in the (i)–(t) curves. There are three criteria for the NGM: (a) instantaneous (IN) or progressive (P); (b) one-dimensional (1D), two-dimensional (2D), or three-dimensional (3D) nucleation; and (c) controlled by diffusion or charge transfer. Depending on the type of NGM, the current follows a power-type relationship with time. The type of NGM can be determined from the plot of (i) versus t^x, where x: $-(1/2)$, $(1/2)$, 1, 2, 3, and $(3/2)$, finding which superscript gives linear relationship with respect to (i).[20–23] NGM can only be determined when Region II is well defined. In PPs, $x = 1$, indicating that the NGM is instantaneous, two-dimensional nucleation (IN2D), and controlled by charge transfer.[10] In PPys, except from $PPy_{0.84}$ (which do not appear in Region II), $x = -(1/2)$, indicating that the NGM is IN2D controlled by diffusion with no interactions between the growing centers.[20] In copolymer $(PP\text{-}PPy)_{0.86}$, $x = (1/2)$, indicating that the NGM is IN2D controlled by diffusion but with interactions between the growing centers (nuclei).[20] Thus, the growth of the above-mentioned films takes place in two dimensions (2D) as layer by layer, that is, growing only in parallel direction.[20] This way of growth is very important for the quality of the films as it leads to a compact film, which is in contrast to the 3D growth (not observed in the films synthesized) that leads to loose, powder-like films.[20] For the other copolymers, the NGM could not be determined as Region II is not present. Comparison of the electropolymerization mechanism of the copolymers based on Biph and Py (PP-PPy) with these based on Biph and thiophene (PP-PTh),[10] the latter do not show Region I, indicating that the nucleation starts immediately. On the other hand, (PP-PPy) copolymers do not show Region II, except from $(PP\text{-}PPy)_{0.86}$, and Region III, indicating that the nucleation phenomena are of minor importance and thus the growth of the film starts immediately.[24]

Structural characterization of the copolymers

Figure 3 shows the FTIR spectra of the copolymer $(PP\text{-}PPy)_{0.82}$, and for comparison reason, the FTIR spectra of the homopolymers $PP_{1.80}$ and $PPy_{0.84}$ are

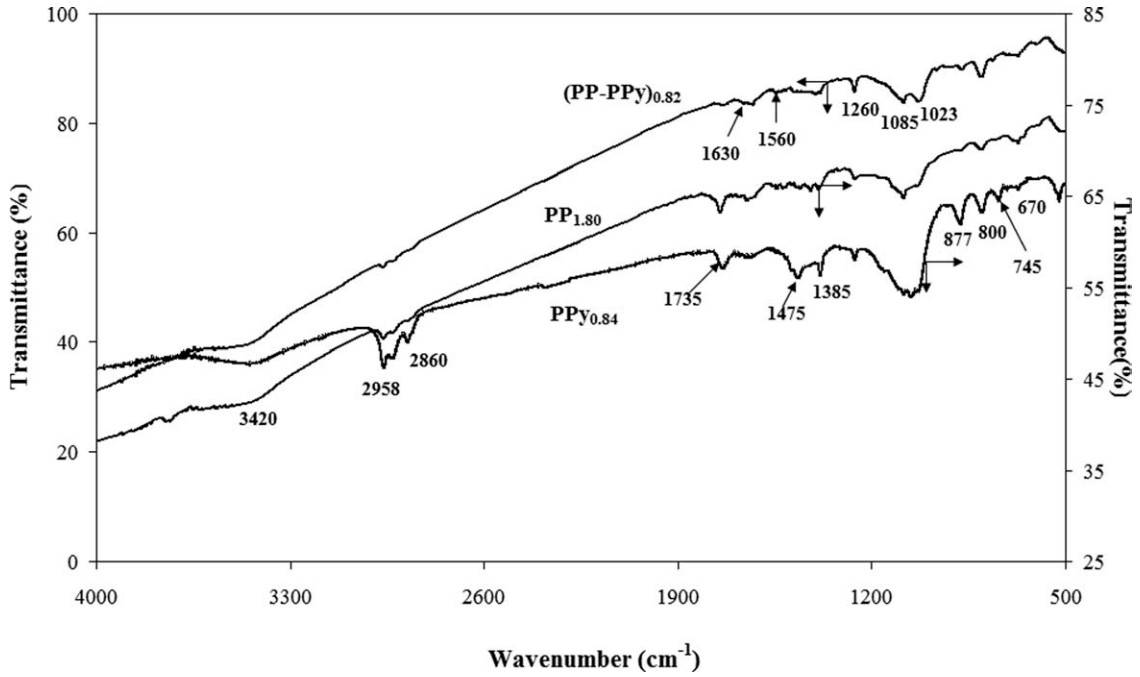

Figure 3 FTIR spectra of homopolymers $PP_{1.80}$ and $PPy_{0.84}$ and copolymer $(PP\text{-}PPy)_{0.82}$ (for the codes, see Table I).

also shown. The various bands of the copolymers and the homopolymers were attributed to chemical bonds according to the literature for the PPs[8–10] and PPys.[25–27] The band at about 3400 cm^{-1} is attributed to the N—H bending vibrations due to Py structural unit,[25] and the bands at 2960 and 2860 cm^{-1} are attributed to the CH_2 aliphatic parts. The bands at around 1630, 1570, 1480, and 1400 cm^{-1} are associated with the aromatic ring (Py or/and Biph ring). The broad absorption band at 1600 cm^{-1} is particularly strong if a further conjugation with aromatic rings takes place. Based on the literature,[28,29] the band at 1570 cm^{-1} is attributed to quinoid structures and the band at 1480 cm^{-1} to benzenoid structures. The copolymers also exhibit the characteristic band of C—N at 1480 and 1260 cm^{-1} due to the Py unit.[25] At 1030 cm^{-1}, the copolymers exhibit a band due to the overlapping of C—H deformation vibrations and N—H bending vibrations. Moreover, the copolymers exhibit the bands of various C—H vibrations at around 1085 and 1030 cm^{-1} ("in-plane" bending vibrations), 875 and 800 cm^{-1} ("out-of-plane" bending vibrations), 745 cm^{-1} (bending vibrations), and 670 cm^{-1} (deformation vibrations). The band at 1740 cm^{-1} corresponds to C—O substitution and specifically to vibration of C=O of pyrrolidinone[27]:

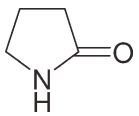

The FTIR spectra of the copolymers cannot confirm that they are indeed copolymers, because the characteristic bands of both the homopolymers appear in the same regions. To confirm that the films formed were copolymers, the solubility of both homopolymers and copolymers was tested in various common solvents (i.e., Et, Me, Ac, NMP, THF, DMF, BzCl, and DMSO). It was found that PPs are totally soluble in NMP and totally insoluble in all other solvents, where PPys are totally insoluble in all solvents studied. Copolymers are partially soluble in DMF and DMSO and totally insoluble in all other solvents. The soluble fraction of polymers (in % w/w) to the total amount of polymer is presented in Table I. The solubility behavior of the copolymers differs from that of the homopolymers, indicating that their structure also differs. Based on the X-ray diffraction analysis diffractograms, the degree of crystallinity, x_c (%), was determined, and these values are also presented in Table I. The PPs synthesized are totally amorphous, whereas the PPys have low crystallinity (except from $PPy_{0.84}$). Correspondingly, copolymers have generally low crystallinity. Their degree of crystallinity is in the following order: $(PP\text{-}PPy)_{0.80} > (PP\text{-}PPy)_{0.82} > (PP\text{-}PPy)_{0.84} > (PP\text{-}PPy)_{0.86}$; therefore, by increasing the applied potential of the electropolymerization, less crystalline (or more amorphous) copolymers are synthesized. Moreover, the soluble fraction of the copolymers follows the reverse order than that of crystallinity (i.e., the insoluble fraction is in accordance with the order of the degree of crystallinity) following the general relation between crystallinity and solubility.

Figure 4 shows the TGA curves of the copolymers $(PP\text{-}PPy)_{0.80}$ and $(PP\text{-}PPy)_{0.86}$ and the homopolymers

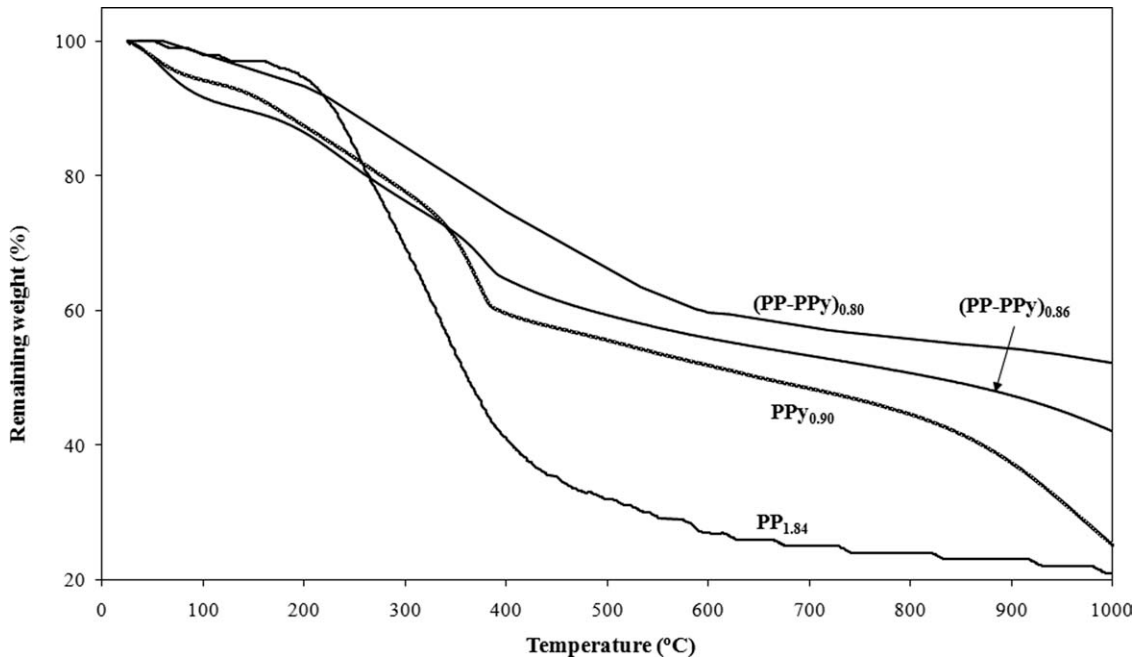

Figure 4 TGA curves of homopolymers $PP_{1.84}$ and $PPy_{0.90}$ and copolymers $(PP\text{-}PPy)_{0.80}$ and $(PP\text{-}PPy)_{0.86}$ (for the codes see Table I; TGA curve of polyphenylene $PP_{1.84}$ is from Ref. 10).

$PP_{1.84}$ and $PPy_{0.90}$. The weight loss of the polymers can be analyzed in three regions: (A) up to 200°C; (B) from 200 up to 500°C; and (C) from 500 up to 1000°C. The weight loss (%) of polymers $PP_{1.84}$, $PPy_{0.90}$, $(PP\text{-}PPy)_{0.80}$, and $(PP\text{-}PPy)_{0.86}$ in Region A is 6.0, 12.6, 6.7, and 13.6%, respectively. Likewise, in Region B, the weight loss is 62.5, 31.8, 27.0, and 27.2%, respectively, and in Region C, the weight loss is 10.5, 30.4, 14.1, and 17.2%, respectively. $PP_{1.84}$ is almost stable up to 200°C and then up to 500°C exhibits an abrupt weight loss (62.5%). This abrupt weight loss proves that $PP_{1.84}$ contains not only para-linkages but also meta-linkages between Biph units. Indeed, poly(*p*-phenylene) having only para-linkages exhibits a very low weight loss (25% for undoped and 40% for the doped, heated up to 1000°C).[9] The weight loss of $PPy_{0.90}$ begins at 80°C and continues up to 1000°C, exhibiting lower weight loss than PP. The copolymers have lower total weight loss than the homopolymers and they are more stable up to 1000°C. This is due to the incorporation of Biph units (consisting of two aryl rings) that stabilize the segments of Py units.

Combining the results of TGA, crystallinity, and solubility by complementarily using the EDAX results, a possible model structure for copolymers $(PP\text{-}PPy)_{0.80}$ and $(PP\text{-}PPy)_{0.86}$ is proposed [Scheme 1(c,d)], as well as for the corresponding homopolymers [Scheme 1(a,b)]. In PP homopolymer [Scheme 1(a)], the meta-linkages are more than para-linkages, leading to a totally soluble polymer, opposite to PPy homopolymer [Scheme 1(b)]. PPy has almost excessive α,α′ linkages (i.e., 2,5 linkages) between two neighboring Py structural units, which is a very stable structure that resembles the para-linkages of six carbon rings of poly(*p*-phenylenes). When compared with $(PP\text{-}PPy)_{0.86}$, copolymer $(PP\text{-}PPy)_{0.80}$ has lower soluble fraction, higher crystallinity, and higher thermal stability, containing more para-linkages than meta-linkages [Scheme 1(c)]. On the other hand, copolymer $(PP\text{-}PPy)_{0.86}$ contains more meta-linkages than para-linkages [Scheme 1(d)].

Morphology and elemental analysis of the copolymers

Figure 5 presents the SEM micrographs of copolymers and homopolymers. $PP_{1.80}$ has a morphology of globular aggregates with size between 3.5 and 6 μm [Fig. 5(a)]. $PP_{1.84}$ has a sponge-like structure with small-sized aggregates [smaller than 1 μm; Fig. 5(b)]; however, it appears more compact than $PP_{1.80}$. PPys [Fig. 5(c,d)] have fibrillar morphology with pores. $PPy_{0.84}$ has small round-shaped pores (with diameter between 2 and 2.8 μm), whereas $PPy_{0.90}$ has many irregularly shaped pores with large size (with diameter 7.5–9.5 μm). The copolymer $(PP\text{-}PPy)_{0.80}$ has a morphology of globular aggregates with medium size between 5.5 and 6.5 μm, but appears compact. On the other hand, $(PP\text{-}PPy)_{0.86}$ has fibrillar morphology with many round-shaped pores (with diameter between 3 and 5.8 μm). It can be deduced that the electropolymerization potential strongly affects the morphology of the copolymer

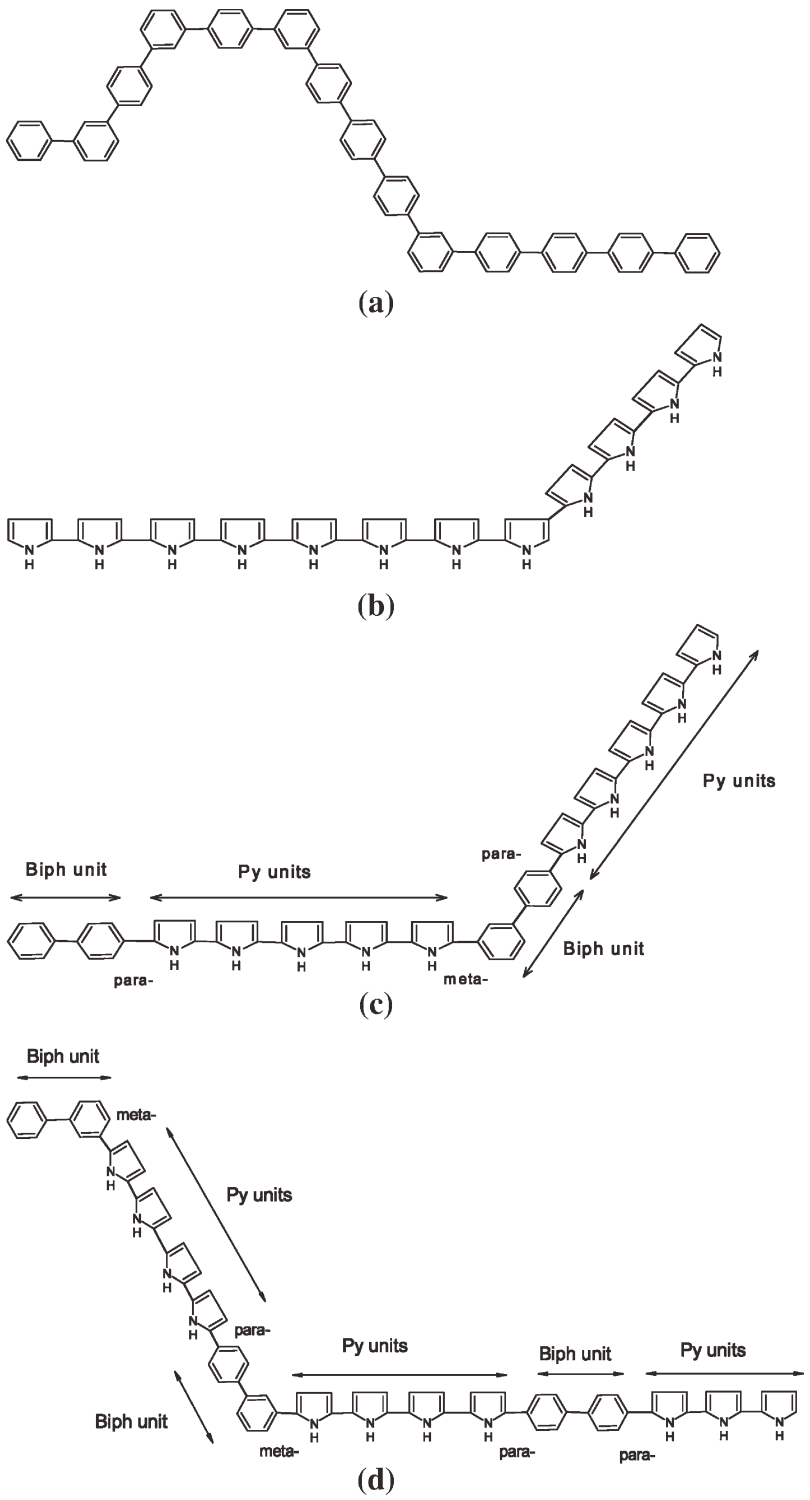

Scheme 1 Model structure for (a) homopolymer PP, (b) homopolymer PPy, (c) copolymer $(PP\text{-}PPy)_{0.80}$, and (d) copolymer $(PP\text{-}PPy)_{0.86}$.

films. Moreover, the type of monomers used for the copolymers influence the morphology of the films. For example, by replacing the Py with the thiophene, the copolymers (PP-PTh) have a totally different morphology, with round-shaped cracks or with large-sized aggregates,[10] opposite to (PP-PPy) that have globular or fibrillar morphology.

The EDAX results are presented in Table II. It is noticed that the values of % w/w of carbon, oxygen, fluorine, and nitrogen are the mean values of at least three measurements, and the standard error of the measurements is also presented. From these data, the ratio of structural unit of homopolymers (Biph or Py) per BF_4^- dopant ion (counter ion) was

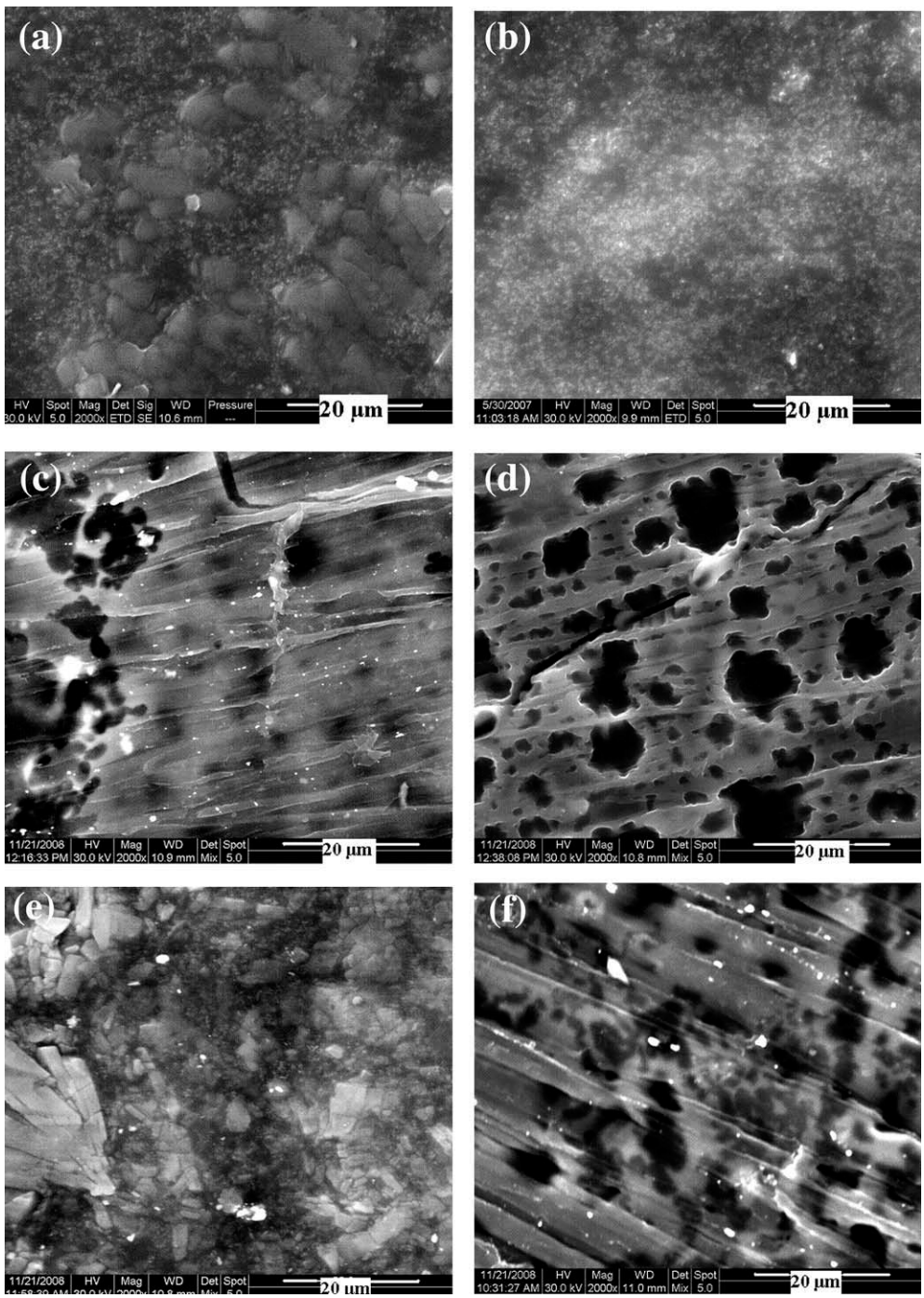

Figure 5 SEM micrographs (×2000) of (a and b) homopolymers $PP_{1.80}$ and $PP_{1.84}$, respectively; (c and d) homopolymers $PPy_{0.84}$ and $PPy_{0.90}$, respectively; (e and f) copolymers $(PP\text{-}PPy)_{0.80}$ and $(PP\text{-}PPy)_{0.86}$, respectively.

calculated, and the results are also presented in Table II. For PPs, the ratio of F/C (w/w) was converted to the molecular ratio of F/C and then (taking into consideration that a dopant anion contains four fluorine atoms) in BF_4^-/C (mol/mol). The latter ratio can be converted to the ratio of structural Biph units per counter ion, taking into consideration that one structural Biph unit contains 12 carbon atoms. Similarly, the ratio of structural Py units (containing one nitrogen atom) per counter ion was calculated. For PPs, it was found that the ratio is between 4.1 ($PP_{1.84}$) and 4.8 ($PP_{1.80}$) structural units per dopant ion.[10] For PPys, it was found that this ratio is $\sim$ 4.0 structural units per dopant ion. For the copolymers, the ratio of structural unit derived from Biph per that derived from Py was calculated,[10,14] and the values are also presented in Table II. For this calculation, only the amounts of carbon and

TABLE II
Energy-Dispersive X-ray Analysis of the Polymers Synthesized

Code of polymers	Elemental analysis (% w/w)				Ratio		Ratio of structural unit per counter ion	Ratio of structural units into the copolymers
	C	O	F	N	F/C (w/w)	F/N (w/w)		
$PPy_{0.84}$	67.0 ± 2.2	7.2 ± 0.8	14.7 ± 1.0	11.1 ± 1.0	0.22	1.33	Pyrrole units 4.0/1	
$PPy_{0.90}$	68.4 ± 0.4	6.1 ± 0.4	14.6 ± 0.6	10.9 ± 0.3	0.21	1.34	Pyrrole units 4.1/1	
$(PP\text{-}PPy)_{0.80}$	68.4 ± 6.9	2.4 ± 0.9	17.1 ± 5.3	12.1 ± 0.5	0.25	1.41		Biph/Py = 1/4.8
$(PP\text{-}PPy)_{0.86}$	69.3 ± 2.1	4.6 ± 3.6	15.4 ± 1.2	10.7 ± 0.3	0.22	1.43		Biph/Py = 1/3.4

For homopolymers $PP_{1.80}$ and $PP_{1.84}$, the ratio of biphenyl structural units per counter ion is 4.8/1 and 4.1/1, respectively.[10]

nitrogen are necessary, and therefore, the amounts of oxygen and fluorine were omitted and the ratio of carbon to nitrogen was expressed in percentage rate (% w/w). This ratio was converted to molecular ratio (mol/mol) and then the structural units of Biph and Py contained in the copolymers was calculated. In $(PP\text{-}PPy)_{0.80}$, the ratio of structural units of Biph/Py was 1/4.8 and in $(PP\text{-}PPy)_{0.86}$ was 1/3.4. Thus, copolymers contain more structural units of Py than Biph. This is a result of the faster electropolymerization of Py when compared with that of Biph, as observed from the much lower oxidation potential of the former. This procedure will be discussed below.

PPys contain defects due to the incorporation of oxygen into the Py structural unit during the electropolymerization[27] and defects of alkyl terminating groups, that is, Py-(C_4H_9), bonded to end Py structural unit of the macromolecule.[30] These alkyl groups originating from the supporting electrolyte are formed at the cathode and then, by side reactions, are bonded with the oxidized polymer at the anode. Moreover, the dopant anion $(BF_4)^-$ is associated with the polymeric backbone, leading to structural modifications. Therefore, not all the percentage amount of carbon determined by any elemental analysis (e.g., conventional elemental analysis and EDAX) belong to the structural units of Py and Biph. However, the percentage amount of nitrogen belongs exclusively to the Py structural units and, therefore, it can be used to determine these units contained into the macromolecules of the copolymers. On the other hand, the determination of the Biph structural units contained into the macromolecules of the copolymers is based on the percentage amount of the rest carbon (by subtracting the carbon of the Py structural units, previously determined by nitrogen) and it contains the error of the formed structural defects. The determination of such defects consists of a very difficult analysis problem of the polymers. Therefore, the values of the ratio of structural units into the copolymers (Table II) should not be considered as absolute values. However, their relative meaning has very useful practical significance.

Electrical conductivity and energy gap of the copolymers

The electrical conductivity (σ) of the films is presented in Table III. The highest conductivity for PPs is exhibited in $PP_{1.84}$ (0.62 S/cm), that is, film synthesized in a potential higher than E_{ox} of Biph. Similarly, the highest conductivity for PPy is

TABLE III
Values of E^{ox}_{onset}, E^{red}_{onset}, E_{HOMO}, E_{LUMO}, and E_g of the Films and the Electrical Conductivity of Polymeric Films

Code of polymers	E^{ox}_{onset} (V)	E_{HOMO} (eV)	E^{red}_{onset} (V)	E_{LUMO} (eV)	E_g (eV)	Electrical conductivity σ (S/cm)
$PP_{1.80}$	+0.55	−4.95	−0.98	−3.42	1.53	2.4×10^{-2}
$PP_{1.82}$	+0.58	−4.98	−0.97	−3.43	1.55	1.3×10^{-2}
$PP_{1.84}$	+0.62	−5.02	−0.87	−3.53	1.49	6.2×10^{-1}
$PPy_{0.84}$	+0.12	−4.52	−1.09	−3.31	1.21	8.0×10^{-1}
$PPy_{0.86}$	+0.25	−4.65	−1.02	−3.38	1.27	5.1×10^{-1}
$PPy_{0.88}$	+0.20	−4.60	−1.05	−3.35	1.25	6.0×10^{-1}
$PPy_{0.90}$	+0.15	−4.55	−1.09	−3.31	1.24	6.5×10^{-1}
$(PP\text{-}PPy)_{0.80}$	+0.10	−4.50	−1.10	−3.30	1.20	8.7×10^{-1}
$(PP\text{-}PPy)_{0.82}$	+0.20	−4.60	−1.10	−3.30	1.30	4.2×10^{-1}
$(PP\text{-}PPy)_{0.84}$	+0.10	−4.50	−1.30	−3.10	1.40	1.0×10^{-1}
$(PP\text{-}PPy)_{0.86}$	+0.03	−4.43	−1.30	−3.10	1.33	3.0×10^{-1}

E^{ox}_{onset}: onset potential for p-doping, vs. SCE; E^{red}_{onset}: onset potential for n-doping, vs. SCE; E_{HOMO}: energy level of highest occupied molecular orbital (HOMO), i.e., of valence band; E_{LUMO}: energy level of lowest unoccupied molecular orbital (LUMO), i.e., of conduction band; E_g: energy gap. Results of polyphenylenes $PP_{1.80}$, $PP_{1.82}$, and $PP_{1.84}$ are taken from Ref. 10.

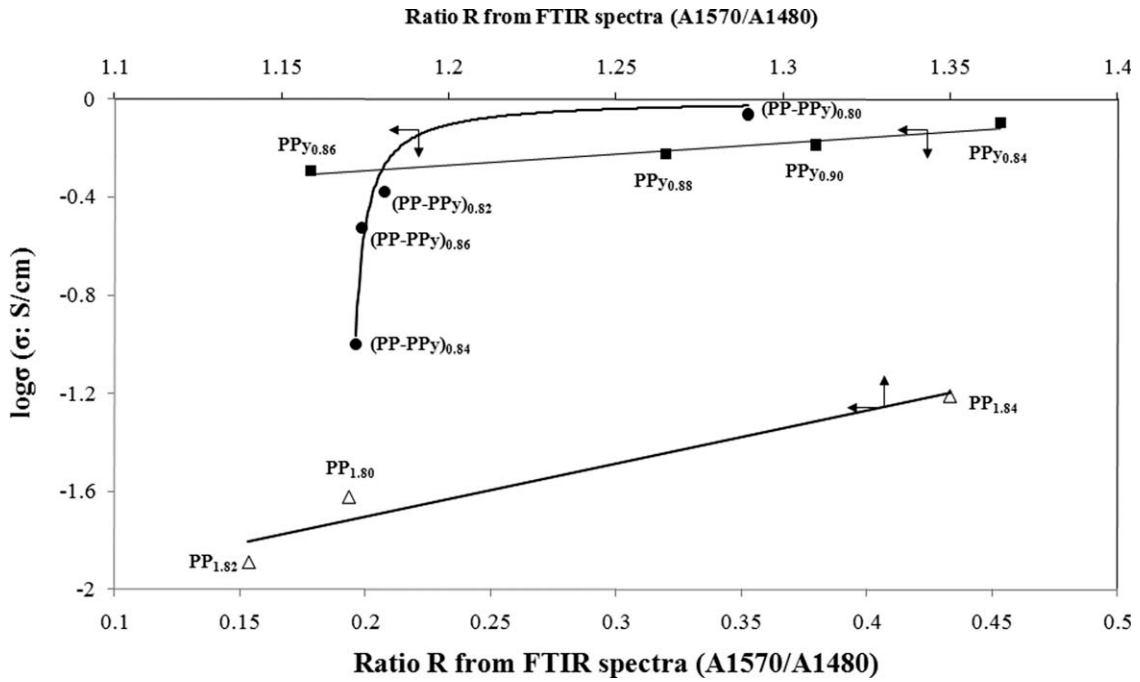

Figure 6 Electrical conductivity of polymer films versus the ratio R of the peak area of the quinoid to benzenoid (for the codes see Table I).

exhibited in $PPy_{0.84}$ (0.8 S/cm), again synthesized in a potential higher than E_{ox} of Py. Contrarily to the homopolymers, the highest conductivity for the copolymers is exhibited in $(PP\text{-}PPy)_{0.80}$ (0.87 S/cm), which is synthesized in the E_{ox} of the monomer system. By comparing these copolymers with those of Biph with thiophene (PP-PTh),[10] it is shown that their electrical conductivity is in the same order of magnitude.

The electrical conductivity of the copolymers can be correlated to the morphology of the films and to their ratio of Biph to Py structural units (calculated from EDAX). Likewise, the electrical conductivity of the homopolymers can be correlated to the morphology of the films and to their ratio of structural units per counter ion (calculated from EDAX). For all polymers, the highest conductivity appears in the more compact films. This can be explained considering that the more compact films have a more extensive and continuous network of active paths, which facilitate the charge transfer. In homopolymers, the highest conductivity appears in polymers having the lowest ratio of structural units per counter ion, which indicates that they are more doped.[12] Considering that PPys generally have higher conductivity than PPs, by increasing the content of Py units, it is expected that the conductivity of the copolymers would increase. Indeed, in copolymers, the higher conductivity appears in polymers having the higher ratio of Py units.

As already described in the literature,[28] the electrical conductivity can be correlated with the structure of the polymers. The ratios R of the peak area of the quinoid (A_{1570}) to benzenoid (A_{1480}) absorption bands of the synthesized polymers were calculated and plotted versus the logarithm of electrical conductivity (log σ; Fig. 6). For the copolymers, the electrical conductivity increases by increasing R following a ratio type relationship, whereas for the homopolymers, it follows a linear increase relationship. This proves a direct correlation between electrical conductivity and R, that is, the electrical conductivity increases by increasing the quinoid structures in the macromolecules. In the copolymers based on Biph and thiophene (PP-PTh), the R increases with the conductivity following a linear relationship, indicating a different conductivity behavior.

Figure 7 shows the cyclic voltammogram of the blank solution and of the copolymer film $(PP\text{-}PPy)_{0.82}$. In the case of blank solution, no peaks are observed, and the current is very low. Thus, any peaks that appear in the case of the films are due to the polymers. The onset potentials of oxidation and reduction for the p-doping (E^{ox}_{onset}) and n-doping (E^{red}_{onset}), respectively, were determined graphically.[31,32] Then, from the equations given by de Leeuw et al.,[31,32] E_{HOMO}, E_{LUMO}, and E_g were calculated as follows:

$$E_{HOMO} = -e(E^{ox}_{onset} + 4.4) \quad (2)$$

$$E_{LUMO} = -e(E^{red}_{onset} + 4.4) \quad (3)$$

$$E_g = e(E^{ox}_{onset} - E^{red}_{onset}) \quad (4)$$

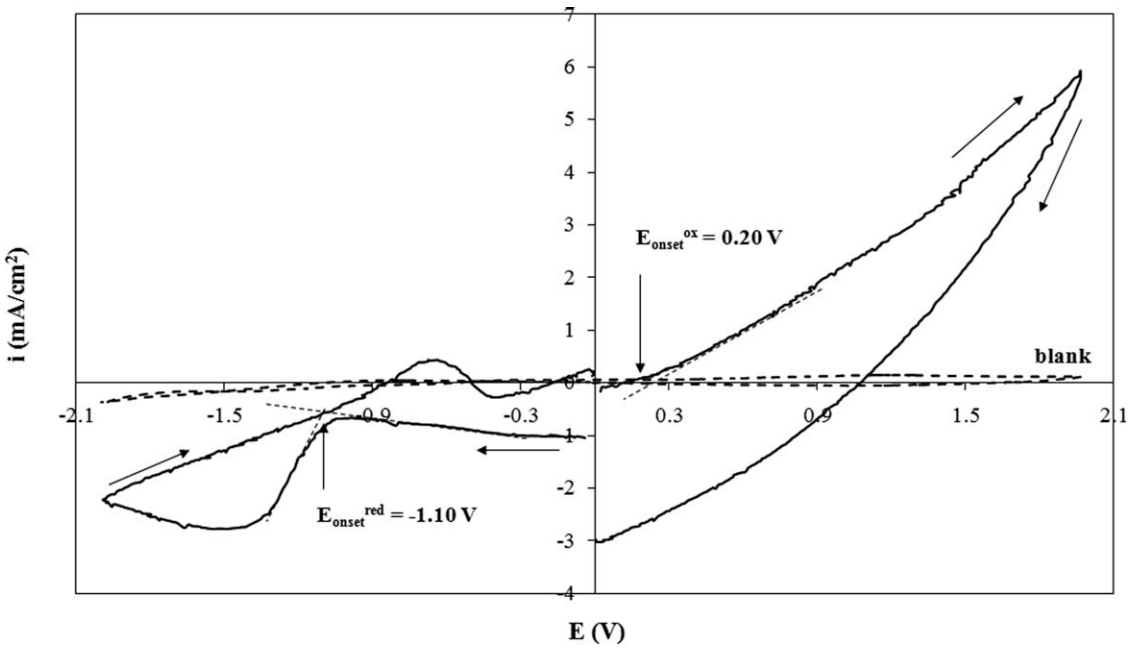

Figure 7 Cyclic voltammogram of blank solution and of the copolymer film $(PP\text{-}PPy)_{0.82}$ (for the code see Table I) with solution of 0.1*M* $TBABF_4$ in ACN, scan rate = 100 mV/s, for the determination of the onset potential for p- and n-doping.

where E^{ox}_{onset}: onset potential for p-doping, vs. SCE; $E^{red.}_{onset}$ onset potential for n-doping, vs. SCE; E_{HOMO}: energy level of HOMO, that is, of valence band; E_{LUMO}: energy level of LUMO, that is, of conduction band; and E_g: energy gap.

The values of E^{ox}_{onset}, E^{red}_{onset}, E_{HOMO}, E_{LUMO}, and E_g of the homopolymers and the copolymers are summarized in Table III. The E_g of polymers varies from 1.20 up to 1.55 eV, in the range of semiconductors.[33] E_g is reversely proportional to the electrical conductivity, and thus, the polymers with the highest conductivity also had the lowest E_g, that is, $PP_{1.84}$ (1.49 eV), $PPy_{0.84}$ (1.21 eV), and $(PP\text{-}PPy)_{0.80}$ (1.20 eV). According to the literature,[34] materials with values of electrical conductivity higher than 10^{-3} S/cm can be used in batteries, sensors, LEDs, etc. Thus, the copolymer films are suitable candidate materials for this kind of applications.

When compared with the copolymers (PP-PPy) with the copolymers based on Biph with thiophene (PP-PTh),[10] the electropolymerization was carried at potentials ranging between 0.80 and 0.90 V in the former and between 1.80 and 1.90 V in the latter copolymers. In both kinds of copolymers, the highest electrical conductivity (in the order of magnitude of 10^{-1} S/cm) and the lowest band gap (around 1.20 eV) appear in the copolymers synthesized at their lowest polymerization potential (i.e., the oxidation potential, 0.80 V for PP-PPy and 1.80 V for PP-PTh). However, they have different HOMO and LUMO energy levels and, more specifically, the (PP-PPy) has lower energy levels (HOMO and LUMO) than the (PP-PTh). This difference means that the copolymers can be used in different electrooptical applications. For example, the efficiency of an organic solar cell is defined by the function of the p–n diode, which depends on the energy levels of p- and n-type semiconductor materials.[35] Thus, both kinds of copolymers (which are p-type semiconductors) can be combined with corresponding proper n-type semiconductors.

Based on the ratio R of the quinoid to benzenoid rings calculated from FTIR spectra, as well as on the electrical conductivity, on the energy gap values, and on the morphology, the copolymer films can be classified into three groups. The first includes the $(PP\text{-}PPy)_{0.80}$, which has $R = 0.35$, the highest value of conductivity (0.9 S/cm), the lowest energy gap (1.20 eV), and it is compact. The second group concerns the copolymers $(PP\text{-}PPy)_{0.82}$, $(PP\text{-}PPy)_{0.84}$, and $(PP\text{-}PPy)_{0.86}$, having $R \sim 0.20$, conductivity lower than 0.4 S/cm (i.e., about half the value of that of the first group), energy gap $\sim$ 1.35 eV, and they have pores. The third group includes the copolymers synthesized at higher applied potential, that is, at 0.88 and 0.90 V. These copolymers have even lower R values, $\sim$ 0.10, significantly lower conductivity ($\sim 10^{-3}$ S/cm), large energy gap ($\sim$ 1.70 eV), and they are inhomogeneous. It is obvious that the applied potential during electropolymerization affects strongly the properties of the synthesized copolymers. Therefore, the copolymer film synthesized at E_{ox} (0.80 V) has the optimum properties, and as the applied potential increases, the properties of the films diminish.

Stability of the synthesized films

The stability of the films under repetitive potential cycling is very important for practical applications, and thus, cyclic voltammetry was used as a method to evaluate the stability of all the films synthesized. Each film (as deposited film on the electrode) was placed in a solution of ACN with $TBABF_4$ (0.1*M*) and underwent repetitive cyclic potential sweeps with a scan rate of 100 mV/s in two different potential regions (a) broad: from −2 V to +2 V, which is used for the determination of the energy gap, and (b) narrow: from 0 to +2 V, which is used for many applications such as sensors. For every cycle, the anodic and cathodic peaks (i.e., their corresponding potential and current), as well as the total charge of the cycle, were determined. The copolymers of the first and the second group are very stable in both potential regions. Specifically, in the broad potential region, they are stable up to 150 cycles, and the corresponding charge exhibited only a small decrease (less than 0.15% per cycle with reference to the charge of the first cycle). In the narrow potential region, copolymers are even more stable, that is, up to 400 cycles, and the corresponding charge exhibited smaller decrease (less than 0.015% per cycle with reference to the charge of the first cycle). Comparing the stability of (PP-PPy) copolymers with that of copolymers of Biph with thiophene (PP-PTh),[10] the former are profoundly more stable (about twice higher) than the latter. Given that both copolymers (PP-PTh) and (PP-PPy) have high conductivity, for an application where electrochemical stability is required, the latter are more suitable than the former. Concerning the homopolymers (PPs and PPys), they are significantly less stable when compared with the copolymers. Indeed, they are stable only up to 15 cycles in the broad potential region and up to 35 cycles in the narrow one.

CONCLUSIONS

New electrically conducting copolymer films were synthesized by potentiostatic electropolymerization of Biph with Py, having different structure and properties than the corresponding homopolymers. From the current–time curves, it was found that the growth of the copolymer films starts immediately. The copolymers have low crystallinity, partially soluble in DMSO and DMF, and the degree of crystallinity and the insoluble fraction decreases by increasing the applied potential during electropolymerization. The copolymers are more thermally stable than the homopolymers, having lower total weight loss up to 1000°C. The copolymer film synthesized at low potential (E_{ox} = 0.80 V) has globular aggregates and that at high potential (0.86 V) has fibrillar morphology. The copolymers contain more structural units of Py than Biph, in proportion of 1/4.8 or 1/3.4 for the low or the high potential, respectively. Based on the ratio *R* of the quinoid to benzenoid rings calculated from FTIR spectra, as well as on the electrical conductivity (σ) on the energy gap (E_g) values, and the SEM analysis, the copolymers can be classified into three groups. The first includes the $(PP\text{-}PPy)_{0.80}$ synthesized at the lowest potential E_{ox} (0.80 V), having the highest ratio *R* (= 0.35), the highest value of σ (= 0.9 S/cm), the lowest E_g (= 1.20 eV), and has compact morphology. The second group concerns the copolymers synthesized at higher potentials, $(PP\text{-}PPy)_{0.82}$, $(PP\text{-}PPy)_{0.84}$, and $(PP\text{-}PPy)_{0.86}$, having lower *R* (∼ 0.20), lower σ (below 0.4 S/cm), higher E_g (∼ 1.35 eV), and they are less compact with many pores. The third group includes the copolymers synthesized at even higher applied potential (0.88 and 0.90 V), having even lower *R* values (∼ 0.10), significantly lower σ (∼ 10^{-3} S/cm), even higher E_g (∼ 1.70 eV), and they are very porous. The copolymers of the first and the second group are very stable under repetitive potential cycling in both broad and narrow potential regions, that is, up to 150 and 400 cycles, respectively. In conclusion, the applied potential during electropolymerization strongly affects the properties of the synthesized copolymers. Because of the combination of high conductivity, low energy gap, and partial solubility with significant electrochemical stability, these new copolymers are attractive candidates for many applications such as LEDs and sensors.

References

1. Sarac, A. S. In Encyclopedia of Polymer Science and Technology, 4th edition (online); Wiley: New York, 2006, Vol. 6, Chap. Electropolymerization, p. 1.
2. Foot, P. J. A.; Kaiser, A. B. In Kirk-Othmer Encyclopedia of Chemical Technology, online edition; Wiley: New York, 2004, Vol. 7, Chap. Conducting Polymers, p. 513.
3. Wu, J.; Li, Q.; Fan, L.; Lan, Z.; Li, P.; Lin, J.; Hao, S. J Power Sources 2008, 181, 172.
4. Xia, L.; Wei, Z.; Wan, M. J Colloid Interface Sci 2010, 341, 1.
5. Waghuley, S. A.; Yenorkar, S. M.; Yawale, S. S.; Yawale, S. P. Sens Actuators B 2008, 128, 366.
6. Guimard, N. K.; Gomez, N.; Schmidt, C. F. Prog Polym Sci 2007, 32, 876.
7. Zotti, G. In Handbook of Organic Conductive Molecules and Polymers; Nalwa, H. S., Ed.; Wiley: Chichester, 1997, Chap. 4, p. 137.
8. Lacaze, P. C.; Aeiyach, S.; Lacroix, J. C. In Handbook of Organic Conductive Molecules and Polymers; Nalwa, H. S., Ed.; Wiley: Chichester, 1997, Chap. 6, p. 205.
9. Simitzis, J.; Triantou, D.; Soulis, S. J Appl Polym Sci 2008, 110, 356.
10. Simitzis, J.; Triantou, D.; Soulis, S. J Appl Polym Sci 2010, 118, 1494.
11. Kovacic, P.; Jones, M. B. Chem Rev 1987, 87, 357.
12. Zarras, P.; Irvin, P. In Encyclopedia of Polymer Science and Technology, 4th edition (online); Wiley: New York, 2003, Vol. 6, Chap. Electrically Active Polymers, p. 88.

13. Tietje-Girault, J.; Ponce de León, C.; Walsh, F. C. Surf Coat Technol 2007, 201, 6025.
14. Latonen, R. M.; Kvarnström, C.; Ivaska, A. Electrochem Acta 1999, 44, 1933.
15. Blythe, A.R. Electrical Properties of Polymers, Cambridge University Press: Cambridge, 1979.
16. Cervini, R.; Li, X. C.; Spencer, G. W.; Holmes, A. B.; Moratti, S. C.; Friend, R. H. Synth Met 1997, 84, 359.
17. Adamcová, Z.; Dempírová, L. Prog Org Coat 1989, 16, 295.
18. Zotti, G.; Cattarin, S.; Comisso, N. J Electroanal Chem 1987, 235, 259.
19. Diaz, A. F.; Castillo, J. L.; Logan, J. A.; Lee, W. Y. J Electroanal Chem 1981, 129, 115.
20. Vignali, M.; Edwards, R. A. H.; Serantoni, M.; Cunnane, V. J. J Electroanal Chem 2006, 591, 59.
21. Hillman, A. R.; Mallen, E. F. J Electroanal Chem 1987, 220, 351.
22. Soubiran, P.; Aeiyach, S.; Lacaze, P. C. J Electroanal Chem 1991, 303, 125.
23. Bade, K.; Tsakova, V.; Schultze, J. W. Electrochim Acta 1992, 37, 2255.
24. Mandié, Z.; Duié, L.; Kavačiček, F. Electrochim Acta 1997, 42, 1389.
25. Ping, Z.; Nauer, G. E. J Electroanal Chem 1996, 416, 157.
26. Nicho, M. E.; Hu, H. Sol Energy Mater Sol Cells 2000, 63, 423.
27. Migahed, M. D.; Fahmy, T.; Ishra, M.; Barakat, A. Polym Test 2004, 23, 361.
28. Bhadra, S.; Singha, N. K.; Khastgir, D. J Appl Polym Sci 2007, 104, 1900.
29. Sestrem, R. H.; Ferreira, D. C.; Landers, R.; Temperini, M. L. A.; do Nascimento, G. M. Polymer 2009, 50, 6043.
30. Cheung, K. M.; Bloor, D.; Stevens, G. C. Polymer 1988, 29, 1709.
31. Li, Y.; Cao, Y.; Gao, J.; Wang, D.; Yu, G.; Heeger, A. J. Synth Met 1999, 99, 243.
32. Leeuw, D. M.; Simenon, M. M. J.; Brown, A. R.; Einerhand, R. E. F. Synth Met 1997, 87, 53.
33. Neamen, D. A. Semiconductor Physics and Devices: Basic Principles, 3rd ed.; Mc Graw Hill: Boston, 2003.
34. Furukawa, N.; Nishio, K. In Applications of Electroactive Polymers; Scrosati, E. B., Ed.; Chapman and Hall: London, 1993, Chap. 5, p. 150.
35. Facchetti, A. Chem Mater 2011, 23, 733.